Supporting information

pH-Triggered Nanostructural Transformations in Antimicrobial Peptide-Oleic Acid Self-Assemblies

Mark Gontsarik[a,b], *Mahsa Mohammadtaheri*[a],

Anan Yaghmur[b], *Stefan Salentinig*[a]*

[a]Laboratory for Biointerfaces, Department Materials meet Life, Empa Swiss Federal Laboratories for Materials Science and Technology, Lerchenfeldstrasse 5, 9014, St. Gallen, Switzerland

[b]Department of Pharmacy, Faculty of Health and Medical Sciences, University of Copenhagen, Universitetsparken 2, DK-2100 Copenhagen Ø, Denmark.

Dynamic light scattering (DLS) cumulant analysis

The average diffusion coefficient *D* was obtained by the cumulant analysis from the correlation functions.[1] The hydrodynamic radius R_H was deduced from the diffusion coefficient using the Stokes-Einstein equation:

$$R_H = \frac{k_B T}{6\pi\eta D} \quad \text{(eq. SI1)}$$

k_B being the Boltzmann constant, *T* the absolute temperature and η the viscosity of the solvent. The polydispersity index *PDI* of the size distribution is determined from the second cumulant:

$$PDI = \frac{\mu_2}{\bar{\Gamma}^2} \quad \text{(eq. SI2)}$$

μ_2 being the second cumulant and $\bar{\Gamma}$ the mean of the inverse decay time.

Phase indexing and lattice parameter calculations from SAXS data

The curves exhibiting peak spacing of 1, $\sqrt{3}$, $\sqrt{4}$, corresponding to reflections from planes defined by Miller indices *hk* = 10, 11, 20, were attributed to H_2 inverse hexagonal phase and spacing of $\sqrt{3}$, $\sqrt{8}$, $\sqrt{11}$, 4, $\sqrt{19}$, corresponding to reflections from *hlk* = 111, 220, 311, 400, 331 planes, were attributed to *Fd3m* micellar cubic phase. Lattice parameter *a* for the two phases were calculated using:

$$a_{H_2} = \frac{2d}{\sqrt{3}}\sqrt{h^2 + hk + k^2} \quad \text{(eq. SI3)}$$

$$a_{Fd3m} = d\sqrt{h^2 + k^2 + l^2} \quad \text{(eq. SI4)}$$

were *d* is the interplanar distance given by $d = 2\pi/q$.

Fitting of pKa from the ζ –potential measurements

The ζ –potential measurements at different pH values for samples with 0%, 10% and 20% LL-37 in OA were fitted using following equation derived from the Handerson-Hasselbalch relation.

$$\zeta = Z1 + \frac{Z1 - Z2}{10^{(pK_a^{app} - pH) * p} + 1} \quad \text{(eq. SI5)}$$

where the fitting parameters Z1 and Z2 are the bottom and top asymptotes, pK_a^{app} is the apparent pK_a and p is the hill slope.

LL-37 loading in OA at **pH = 7.0** [wt%]	R_H [nm]	PDI
0	133	0.14
5	164	0.20
10	151	0.19
20	190	0.24
30	105	0.35

LL-37 loading in OA at **pH = 7.5** [wt%]	R_H [nm]	PDI
0	129	0.14
5	164	0.20
10	162	0.25
20	105	0.48
30	94	0.50

Table SI1. R_H and PDI values from the cumulant analysis of the DLS data from OA/LL-37 emulsions with varying loading of LL-37 in OA at pH 7.0 and pH 7.5, R_H presented in graphical form in Figure SI2 and SI3, respectively.

10 wt% LL-37 in OA		
pH	R_H [nm]	PDI
6.0	133	0.13
6.5	176	0.19
7.0	151	0.18
7.5	162	0.25
7.7	124	0.44
8.5	73	0.56

30 wt% LL-37 in OA		
pH	R_H [nm]	PDI
6.0	151	0.36
6.5	155	0.32
7.0	105	0.35
7.5	94	0.50
7.7	57	0.51
8.5	31	0.47

Table SI2. R_H and PDI values from the cumulant analysis of the DLS data from OA/LL-37 emulsions at varying pH between 6.0 and 8.5 at constant LL-37 loading of 10 and 30 wt% in OA, R_H presented in graphical form in Figure 4 and SI6, respectively.

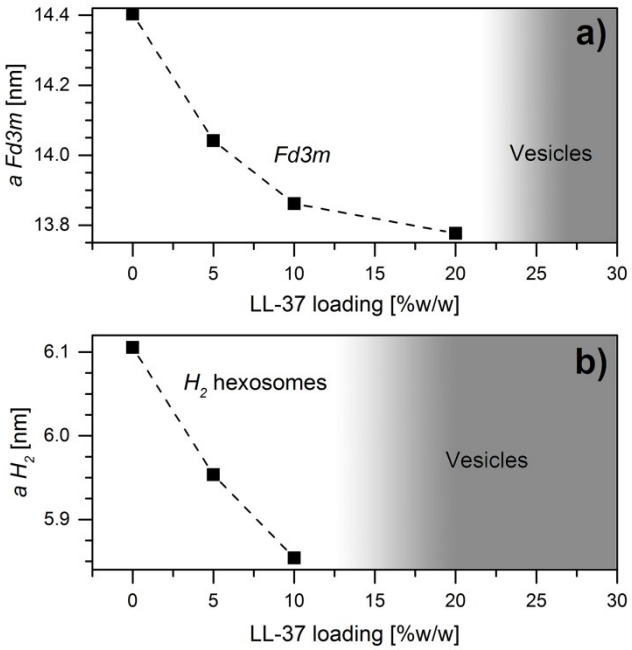

Figure SI1. Calculated lattice parameters for the *Fd3m* and H_2 phase upon increasing the LL-37 concentration relative to OA at a) pH 7.0 and b) pH 7.5. The corresponding SAXS curves are shown in Figure 1 in the main manuscript.

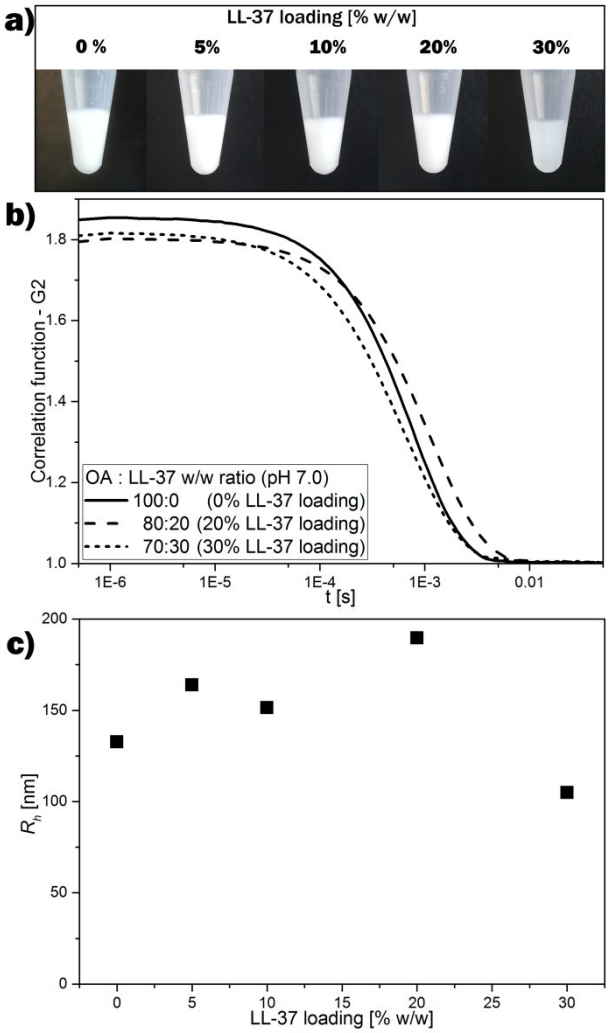

Figure SI2. a) Pictures of the OA/LL-37 dispersions at pH 7.0 with increasing LL-37 concentration relative to OA sowing the decrease in turbidity of the samples with increasing peptide concentration. b) DLS correlation functions for these dispersions; and c) the corresponding R_H values from cumulant analysis of these correlation functions.

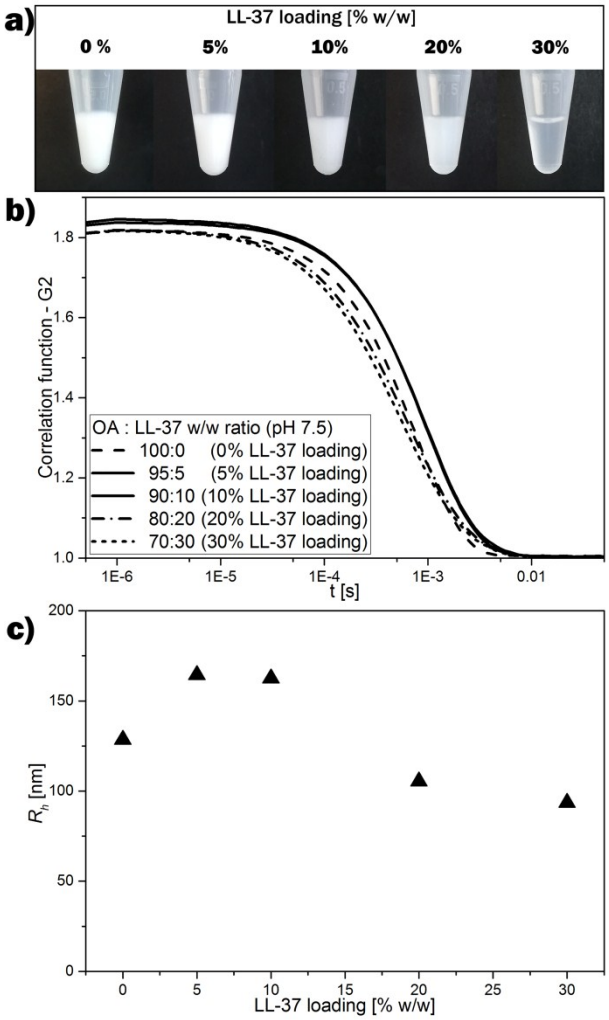

Figure SI3. a) Images of the OA/LL-37 dispersions at pH 7.5 with increasing LL-37 concentration relative to OA showing the decrease in turbidity of the samples with increasing peptide concentration. b) DLS correlation functions for these dispersions; and c) The corresponding R_H values from cumulant analysis of the correlation functions in b)

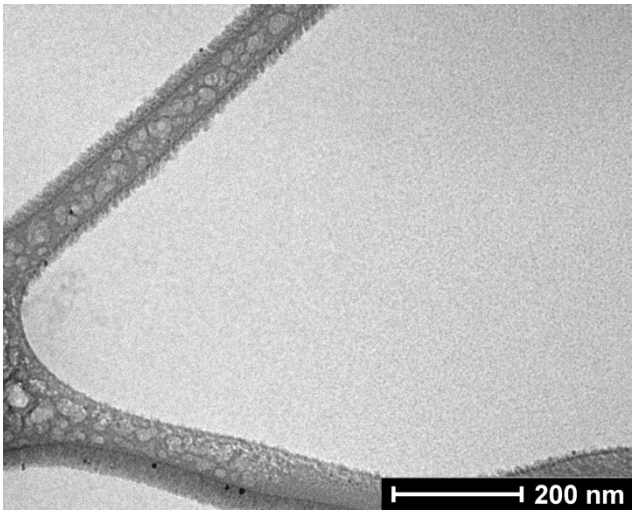

Figure SI4. Representative cryo-TEM image of 10 mg/ml LL-37 in PBS buffer in absence of OA. No Nanoobjects in the 10 nm size range were observed in this system. The dark region in this image is the TEM grid.

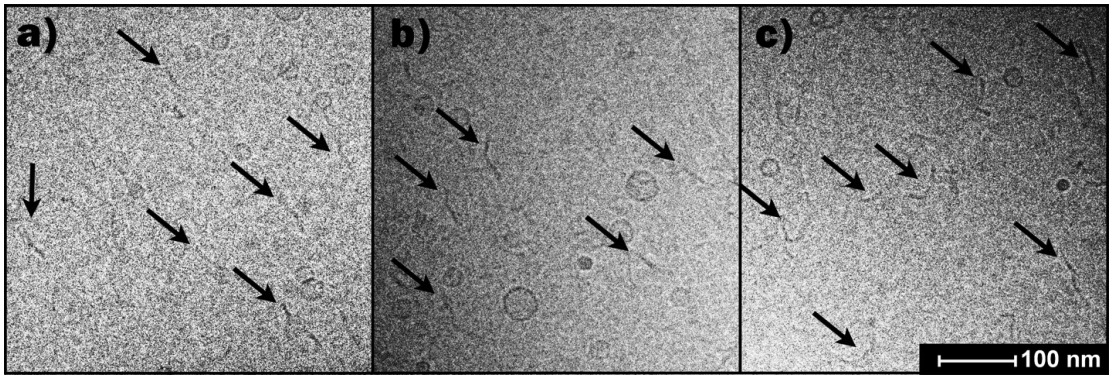

Figure SI5. Representative cryo-TEM image of the OA/LL-37 dispersion containing 30 wt% LL-37 in OA at pH 8.5. Cylindrical micelles and/or bilayer fragments (marked with arrows) coexisting with small vesicles.

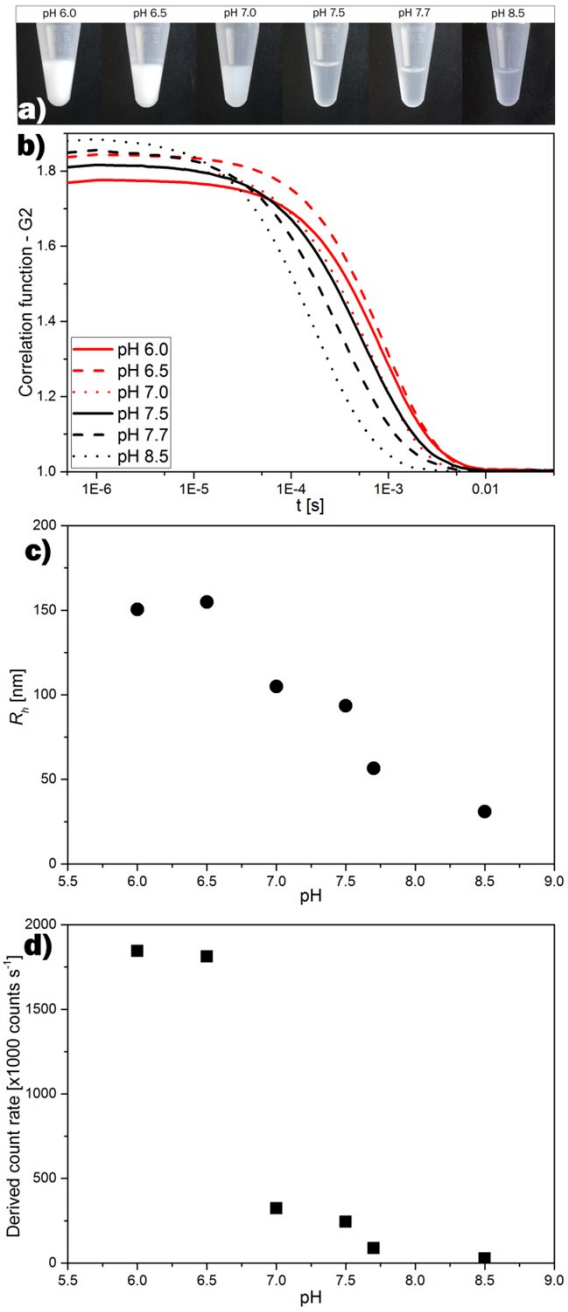

Figure SI6. a) Images of the OA/LL-37 dispersions at 30 wt% LL-37 in OA at different pH values from 6 to 8.5 showing the decrease in turbidity of the samples with increasing pH due to decrease in particle size. b) DLS correlation functions for these dispersions; c) the corresponding R_H values from cumulant analysis of the correlation functions; and d) The corresponding light scattering intensity in this pH range.

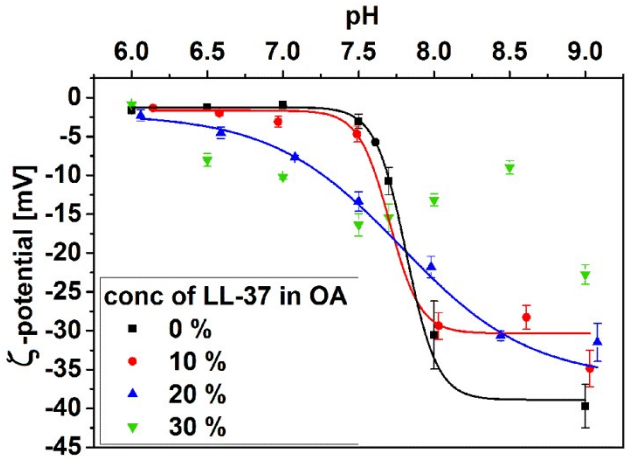

Figure SI7. pH-triggered modifaction of the ζ –potential of OA-based nanocarriers with different LL-37 loading (wt% relative to OA). The pH-induced changes in ζ – potential for samples with 0 wt%, 10 wt% and 20 wt% LL-37 loading in OA were fitted using Eq. SI5. The resulting pK_a^{app} values were 7.82 ± 0.10 (black curve), 7.70 ± 0.18 (red curve) and 7.78 ± 0.12 (blue curve) with increasing LL-37 content.

REFERENCES

1. S. R. Aragón and R. Pecora, *J. Chem. Phys.*, 1976, **64**, 2395.